THE PROTEIN SOCIETY

Resurfaced cell-penetrating nanobodies: A potentially general scaffold for intracellularly targeted protein discovery

Virginia J. Bruce,[1] Monica Lopez-Islas,[1] and Brian R. McNaughton[1,2]*

[1]Department of Chemistry, Colorado State University, Fort Collins, Colorado 80523
[2]Department of Biochemistry & Molecular Biology, Colorado State University, Fort Collins, Colorado 80523

Received 10 February 2016; Accepted 16 March 2016
DOI: 10.1002/pro.2926
Published online 17 March 2016 proteinscience.org

Abstract: By virtue of their size, functional group diversity, and complex structure, proteins can often recognize and modulate disease-relevant macromolecules that present a challenge to small-molecule reagents. Additionally, high-throughput screening and evolution-based methods often make the discovery of new protein binders simpler than the analogous small-molecule discovery process. However, most proteins do not cross the lipid bilayer membrane of mammalian cells. This largely limits the scope of protein therapeutics and basic research tools to those targeting disease-relevant receptors on the cell surface or extracellular matrix. Previously, researchers have shown that cationic resurfacing of proteins can endow cell penetration. However, in our experience, many proteins are not amenable to such extensive mutagenesis. Here, we report that nanobodies—a small and stable protein that can be evolved to recognize virtually any disease-relevant receptor—are amenable to cationic resurfacing, which results in cell internalization. Once internalized, these nanobodies access the cytosol. Polycationic resurfacing does not appreciably alter the structure, expression, and function (target recognition) of a previously reported GFP-binding nanobody, and multiple nanobody scaffolds are amenable to polycationic resurfacing. Given this, we propose that polycationic resurfaced cell-penetrating nanobodies might represent a general scaffold for intracellularly targeted protein drug discovery.

Keywords: nanobody; polycationic resurfacing; supercharging; cell-penetrating

Introduction

Proteins offer unique opportunities as therapeutics and basic research tools. While all small-molecules reported to date modulate a very small percentage of the proteome (~2%)—and only a handful of protein structural classes[1]—the size, functional group diversity, and complex three-dimensional structure of proteins can enable much broader recognition. Moreover, various high-throughput screening and evolution-based methods[2–4] make the discovery of new protein binders simpler than the analogous small-molecule focused process.

One major challenge to the broader use of proteins in biomedical applications is their general inability to efficiently cross the lipid bilayer of mammalian cells and access the cytosol. Thus, most current protein drugs and basic research tools target disease-relevant receptors that reside on the surface of the cell or the extracellular matrix. Efforts to unlock the full potential of proteins in biomedical applications by enabling potent and functional cell penetration have been a major focus of modern biologics research.[5–9] Incorporation of polycationic linkages—such as polyarginine—has previously been described as a means to enable cell penetration of

Additional Supporting Information may be found in the online version of this article.

Grant sponsor: Colorado State University.

*Correspondence to: Brian R. McNaughton, Department of Chemistry, Colorado State University, Fort Collins, CO 80523. E-mail: brian.mcnaughton@colostate.edu

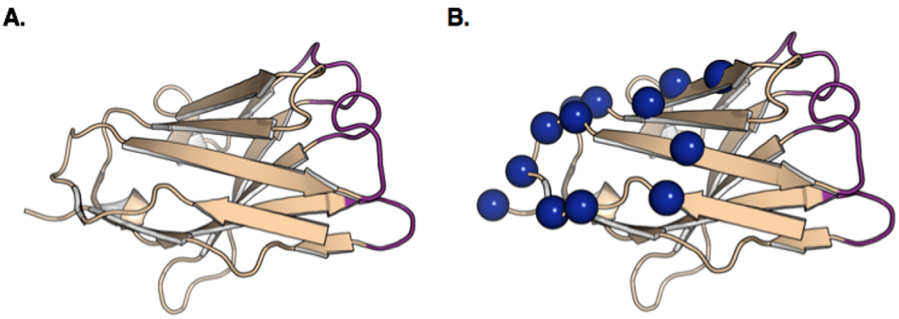

Figure 1. (A) A previously reported nanobody that binds Green Fluorescent Protein (GFP), PDB: 3OGO. This nanobody is referred to as NB1 in this work. Complementarity-determining region (CDR) loops are highlighted in purple. (B) Residues on NB1 that were mutated to either arginine or lysine to generate the resurfaced polycationic nanobody (pcNB1) are highlighted with blue spheres.

various cargo, including proteins.[10] More recently, researchers have used protein engineering to generate polycationic features on the protein surface. For example, Raines and coworkers reported that "arginine grafting"—mutagenesis of clustered solvent exposed amino acids to arginine—enables cellular uptake.[11] In a conceptually similar strategy, Liu and coworkers have shown that protein "supercharging"—extensive mutagenesis of a large number of solvent-exposed residues to positively charged lysine or arginine—results in potent penetration of mammalian cells.[12–14]

While these polycationic resurfacing methods endow potent cell penetration, a major challenge to their broader application is the lack of established and broadly applicable guidelines for this extensive mutagenesis. Relatively little is known about how to dramatically resurface a protein with a polycationic feature in a manner that does not dramatically alter or abolish its utility and/or function (stability, target affinity, expression in *Escherichia coli*). In our experience, even structurally similar proteins respond differently to such extensive mutagenesis, and many proteins of therapeutic interest were not amenable to polycationic resurfacing. Perhaps a simpler approach is to focus effort on developing a single resurfaced polycationic, cell-penetrating, protein scaffold that is stable, expresses in *E. coli*, maintains the function of the original protein, but can be evolved to bind virtually any disease-relevant intracellular target.

Single-domain antibodies derived from camelids, referred to as nanobodies [Fig. 1(A)], have emerged as an alternative to traditional antibodies.[15,16] Features of nanobodies make them well-suited as a general scaffold for protein drug discovery and polycationic resurfacing. In contrast to monoclonal antibodies, nanobodies are produced in large amounts in bacterial expression systems, are small in size (~15 kDa), are usually very stable and often bind their target with excellent affinities ($K_D \sim 1$–100 nM) through interactions involving well-defined antigen binding loops, referred to as the complementarity-determining regions [CDRs, Fig. 1(A), purple].[17] Maturation of amino acids within one or more of the CDR loops by high-throughput screening or evolution-based methods can lead to new proteins that bind virtually any macromolecular target.[18–20]

The structure of nanobodies is highly homologous, and consists of the CDRs, where the nanobody recognizes its target, and a framework region that is rich in β-sheet and loop structure. Researchers have shown that CDR loops can be inserted into a particularly stable nanobody scaffold, resulting in a new nanobody that retains target affinity (based on choice of CDR loops), but has improved stability (based on judicious choice of the nanobody framework).[21] Based on this observation, we hypothesized that if we could engineer polycationic resurfaced nanobody scaffolds, the resulting framework region could likely serve as a generic scaffold for the discovery of cell-penetrating nanobodies that bind and modulate disease-relevant intracellular receptors.

Results and Discussion

Polycationic resurfacing of three previously reported nanobody frameworks

We began with a previously reported nanobody that binds Green Fluorescent Protein [GFP, Fig. 1(A)].[17] Structural analysis of the nanobody that binds GFP (referred to as NB1, herein) revealed a large solvent-exposed surface consisting of a β-sheet and loop structure—within the framework region—that is distinct from the CDR loops. We hypothesized that extensive polycationic resurfacing within this region by mutation of a critical number of residues to arginine (R) or lysine (K) [Fig. 1(B), blue spheres] should endow cell penetration. The sequence and mutagenesis of the wild-type nanobody and resurfaced variant is shown in Figure 2(A). Satisfyingly, the polycationic resurfaced GFP-binding nanobody (referred to as pcNB1, herein), which has a theoretical net charge of +14, expresses as a soluble protein

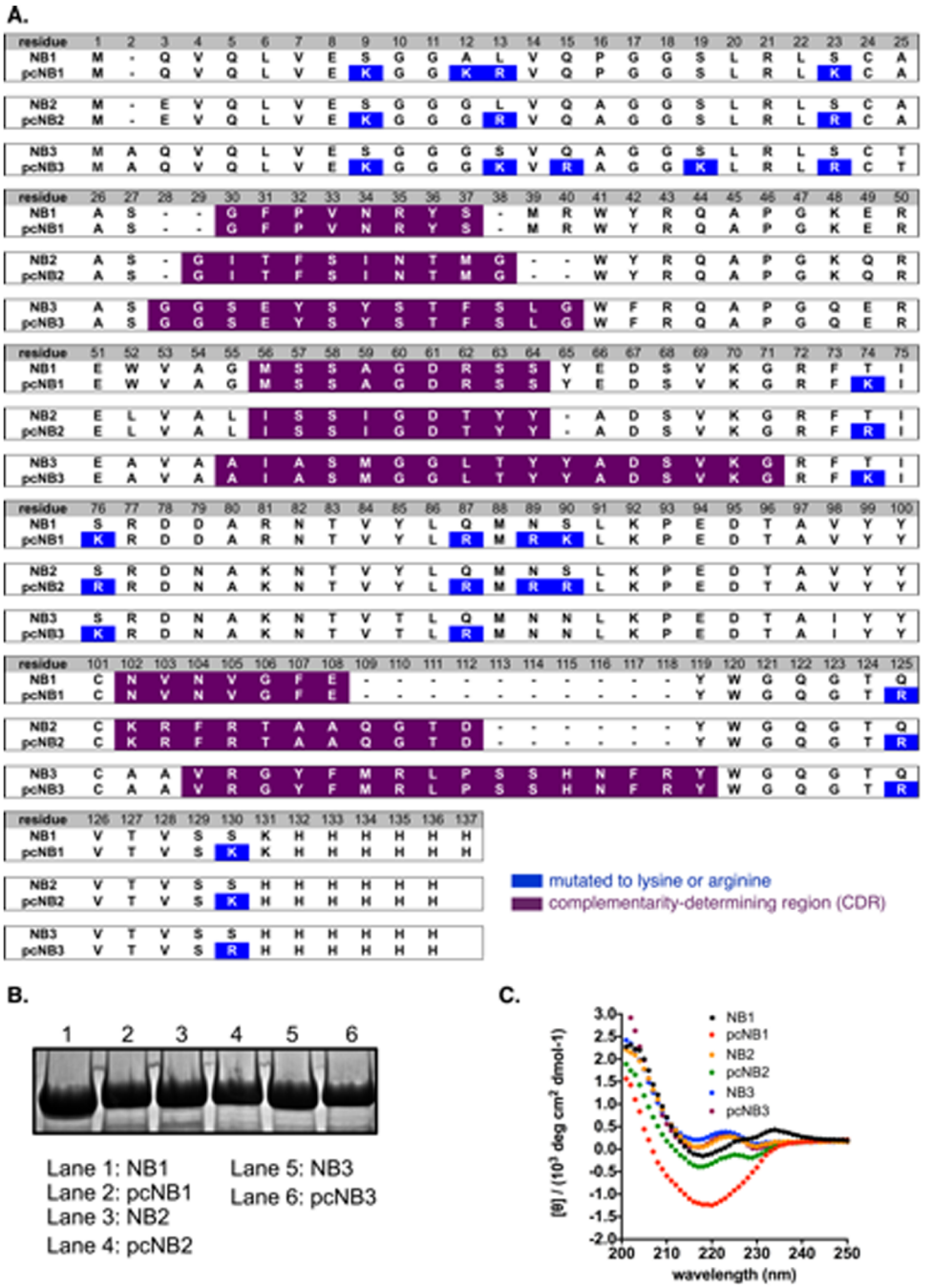

Figure 2. (A) Sequence of wild-type nanobodies (NB1-3) and resurfaced polycationic nanobodies (pcNB1-3) described in this work. (B) PAGE analysis of wild-type and resurfaced polycationic nanobodies described in this work. (C) Circular dichroism spectra of wild-type (NB1-3) and resurfaced polycationic nanobodies (pcNB1-3) described in this work.

in *E. coli* [Fig. 2(B)]. Expanding on this successful result, we performed analogous polycationic resurfacing on two other recently reported nanobodies, which bind HER2[20] or β-lactamase,[22] respectively (referred to as NB2 or NB3, herein). The sequence of the wild-type nanobodies and resurfaced variants is shown in Figure 2(A). While the size and sequence of the CDR loops differ extensively, and small changes in the framework sequence of the wild-type nanobody exist, the resulting polycationic resurfaced nanobodies (referred to as pcNB2 or pcNB3, herein), which have a theoretical net charge of +14 and +15, respectively, express in *E. coli* as soluble proteins [Fig. 2(B)]. Our resurfacing design is summarized as follows: First, we set a goal of generating nanobodies with a theoretical net charge of approximately +15, based on previous cell-penetration studies on supercharged or arginine grafted GFP's.[11,13,23] Second, we focused our mutation on residues that were well within the framework region, and not in or near the CDR loops. Third, we tried to space out mutations, so as to avoid cation/cation repulsion,

which would likely effect protein folding and/or stability. Once candidate residues were identified, based on the above criteria, we considered whether a mutation should result in installation of an arginine or lysine. Since arginine results in better cell surface binding, and cell-penetration,[10] compared to lysine, we favored mutation to arginine, unless the size of neighboring residues suggested that mutation to the relatively large arginine would potentially result in steric clashing. Interestingly, given this relatively simplistic resurfacing design, our initial attempt at polycationic resurfacing was successful for all three nanobody scaffolds. Since analogous attempts to resurface other protein scaffolds are often unsuccessful, in our experience, we conclude that nanobodies may be particularly amenable to such polycationic resurfacing.

Polycationic resurfacing does not alter structure, but does endow internalization of mammalian cells

We next assessed structural features of the wild-type and resurfaced nanobodies by circular dichroism. All nanobodies examined—wild-type and resurfaced variants—have a circular dichroism spectra similar to a previously reported nanobody[24] [Fig. 2(C)]. Collectively, expression of all resurfaced proteins in a soluble form, and similarities in the circular dichroism spectra of the wild-type and mutated variants, suggest that no dramatic structural changes occur as a result of polycationic resurfacing.

To determine uptake efficiency we fused each of our polycationic resurfaced nanobodies to GFP and measured uptake by flow cytometry. 3T3 cells were first treated with 10–500 nM polycationic resurfaced nanobody-GFP fusion, then washed with a phosphate buffered saline solution containing 20 U/mL heparin sulfate—which has been previously shown to remove cell surface bound protein especially supercharged proteins.[6,7,12–14,23] Following treatment with trypsin, which has also been shown to remove and/or degrade surface bound protein,[25] intracellular levels of nanobody-GFP was measured by flow cytometry. For each resurfaced nanobody we observed a concentration-dependent increase of internalized fusion protein, as seen in Figure 3(A–C). In contrast, fusion proteins composed of the wild-type protein and GFP do not appreciably penetrate 3T3 cells [Fig. 3(A–C)]. Internalization was further analyzed by fluorescence microscopy [Fig. 3(D–F)]. Significant levels of each resurfaced nanobody-GFP fusion protein were observed in 3T3 cells, following the above described washing conditions to remove cell surface-bound protein.

Polycation resurfaced nanobodies access the cytosol of mammalian cells

Interestingly, internalized arginine grafted GFP and supercharged GFP appear as punctate foci in fluorescence microscopy images[11,14] (see Fig. S4 Supporting Information)—suggesting encapsulation within endosomes. However, the resurfaced nanobody-GFP fusions do not appear as such, suggesting that appreciable amounts of these internalized nanobodies might access the cytosol. This is critical, since the discovery of future cell-penetrating nanobodies based on these scaffolds would need to access the cytosol in order to engage therapeutically-relevant intracellular targets. This important aspect of cell uptake was further analyzed using a previously described method.[26,27] 3T3 cells were first treated with 250 nM nanobody-GFP or polycationic resurfaced nanobody-GFP fusions, then washed as described above to remove cell surface bound protein. Cells were then lysed with a solution containing digitonin—which breaks the cell surface lipid bilayer, but not endosomes. The cellular location of each internalized fusion protein (cytosolic or endosomal) was then assessed by Western blot, using an anti-GFP antibody (a marker for internalized fusion protein), anti-Erk 1/2 antibody (a marker for the cytosol) or anti-Rab5 antibody (a marker for endosomes). No appreciable amount of GFP or wild-type nanobody-GFP fusion is found within the cytosolic extraction [following cell lysis with digitonin, Fig. 3(G), lanes 2–5], and no appreciable amount of Rab5 is observed (indicating that the lysis does not contain endosomes). In contrast, internalized resurfaced nanobody-GFP fusions appear in the cytosol—in the fraction that tests positive for the cytosolic marker Erk 1/2 but does not have any appreciable amount of the endosome marker Rab5 [Fig. 3(G), lanes 6–8]. Thus, the polycationic resurfaced protein is capable of dragging another protein (GFP) into the cytosol of a mammalian cell.

Fusion to GFP is not required for polycationic resurfaced nanobodies to penetrate mammalian cells and access the cytosol. The same assay was repeated, but cells were incubated with 500 nM wild-type nanobodies or polycationic resurfaced nanobodies with a minimal His_6 tag (for purification and identification by Western blot). As before, wild-type nanobodies do not appear in the cytosolic fraction [Fig. 3(H), lanes 2–4]. In contrast, we observe appreciable levels of the His_6 labeled polycationic resurfaced nanobodies in the cytosolic portion of cell lysate [which stains for cytosolic markers Erk 1/2, Fig. 3(H), lanes 5–7]. As a positive control, when cells are lysed with RIPA buffer, which breaks apart the lipid bilayers of both the cell surface and endosomes, we observe a protein marker for endosomes [Rab5, Fig. 3(I)].

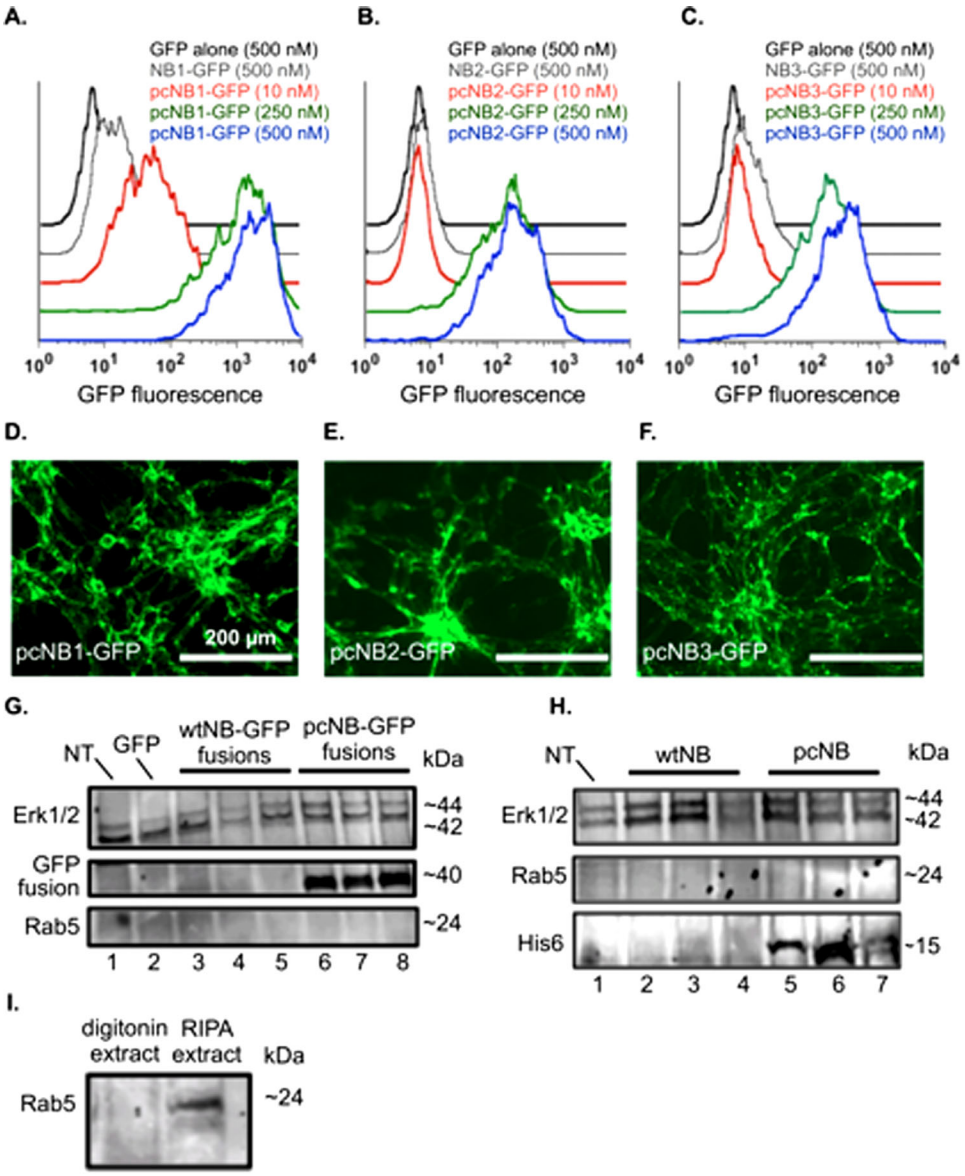

Figure 3. (A–C) Flow cytometry data that supports concentration-dependent uptake of resurfaced polycationic nanobody-GFP fusion proteins, but not GFP alone (black line) or wild-type nanobody-GFP fusion (gray line). Red line = 10 nM treatment; green line = 250 nM treatment; blue line = 500 nM treatment. (D–F) Fluorescence microscopy images of 3T3 cells following treatment with 250 nM resurfaced nanobody-GFP fusions. (G) Western blot analysis of digitonin cell lysate for Erk1/2 (cytosolic marker), GFP (internalized resurfaced nanobody-GFP fusion protein), or Rab5 (endosome marker). Lane 1 = no treatment; lane 2 = wild-type GFP; lane 3 = wild-type NB1-GFP fusion; lane 4 = NB2-GFP fusion; lane 5 = NB3-GFP fusion; lanes 6–8 = polycationic resurfaced nanobody-GFP fusions analogous to lanes 3–5. (H) Western blot analysis of digitonin cell lysate for Erk1/2 (cytosolic marker), His_6 (internalized resurfaced nanobody), or Rab5 (endosome marker). Lane 1 = no treatment; lane 2 = wild-type NB1; lane 3 = NB2; lane 4 = NB3; lanes 5–7 = polycationic resurfaced NB1, NB2, or NB3, respectively. (I) Western blot showing no Rab5 (endosome marker) in cell lysate following digitonin lysis, but in extract following RIPA lysis. For all figures, experiments were run in triplicate and representative data are shown.

Polycationic resurfacing does not alter nanobody function and stability

Having established that the resurfaced nanobodies penetrate mammalian cells and accesses the cytosol, we next explored if this extensive mutagenesis alters function (compared to the wild-type nanobody). This is important, since we want to endow cell penetration, but maintain a structure capable of binding to a target (ultimately an intracellular target following CDR affinity maturation). Among the set of starting nanobodies, retention of function is most easily assessed using the GFP-binding nanobody,[17] since its binding partner (GFP) is easily expressed and observed, and this interaction is particularly well characterized. In order to determine if polycationic resurfaced GFP-binding nanobody (pcNB1 in this

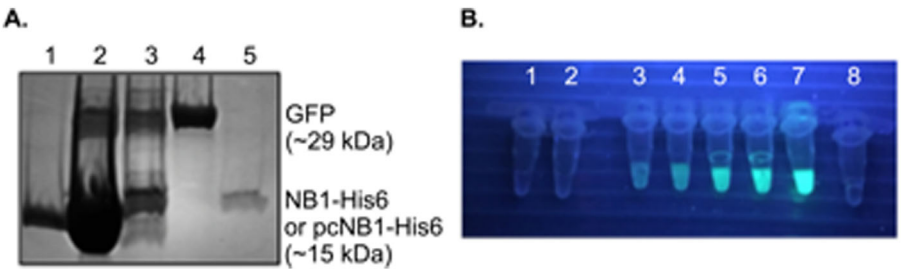

Figure 4. (A) Lane 1: His_6-NB1; Lane 2: co-purification of untagged GFP with His_6-NB1 from *E. coli* cell lysate; Lane 3: co-purification of untagged GFP with His_6-pcNB1; Lane 4: His_6-GFP; Lane 5: His_6-pcNB1. (B) Tube 1: His_6-NB1; Tube 2: His_6-pcNB1; Tubes 3–4: His_6-NB1 and co-eluted GFP; Tubes 5–6: His_6-pcNB1 and co-eluted GFP; Tube 7: His_6-GFP; Tube 8: untagged GFP. For all figures, experiments were run in triplicate and representative data are shown.

work) still binds GFP in a living cell, we co-expressed His_6-labeled NB1 or pcNB1 and untagged GFP in *E. coli* from a pET-DUET plasmid. Following purification on nickel-NTA resin, purified proteins were analyzed by polyacrylamide gel electrophoresis (PAGE) and Coomassie staining. Unsurprisingly, untagged GFP co-purifies with His_6-NB1 [Fig. 4(A), lane 2]. Gratifyingly, untagged GFP also co-purifies with the polycationic resurfaced variant His_6-pcNB1, suggesting that GFP affinity is retained, even in the chemically complex environment of a living cell (*E. coli*). In addition, we performed Isothermal Titration Calorimetry (ITC) experiments to measure affinity between NB1 or pcNB1 and GFP. Because of the high affinity ($K_D \sim 1$ nM), it is difficult to use ITC to measure the equilibrium binding constant with precision. However, as previously reported[17] NB1 binds GFP very tightly, and the resurfaced mutant binds GFP with essentially the same affinity (Fig. S5 Supporting Information).

We next set out to determine how polycationic resurfacing affects protein stability and robustness—important features when considering proteins as basic research tools and therapeutic leads. As previously stated, nanobodies are highly stable and robust proteins. Previous reports have shown that some nanobodies—including the GFP-binding nanobody—can be thermally denatured, but refold when cooled slowly. To see if the polycationic resurfaced GFP-binding nanobody (pcNB1) has the same level of stability and robustness, we tested its ability to recover from thermal denaturation. Both the wild-type His_6-labeled GFP-binding nanobody (His_6-NB1) and His_6-labeled polycationic resurfaced variant (His_6-pcNB1) were heated to 100°C for 2 min, then allowed to cool to room temperature over the course of 2 h. After cooling, the samples were incubated with cell lysate from *E. coli* that expresses recombinant GFP lacking a His_6 label. This solution was then incubated with nickel-NTA resin, the resin was washed, and nickel-bound protein was eluted with imidazole solution. Under these conditions, if His_6-NB1 and His_6-pcNB1 recover from thermal denaturation and regain function (GFP affinity), elution from the column should include both NB1 or pcNB1 and bound GFP. Eluted solutions were analyzed by a long wave (365 nm) hand-held lamp for the presence of GFP. As expected, no appreciable GFP fluorescence is seen when illuminating eluent from nickel-bound His_6-NB1 or His_6-pcNB1 [Fig. 4(B), tubes 1–2]. However, GFP fluorescence (indicating co-elution of the His_6-nanobody and bound GFP) is observed in eluent from nickel-bound His_6-NB1 and untagged GFP [Fig. 4(B), tubes 3–4]. As might be expected with supercharged variants, similar levels of GFP fluorescence is observed in eluent from nickel-bound His_6-pcNB1 and untagged GFP [Fig. 4(B), tubes 5–6]. As a positive control, eluent from nickel-bound His_6-GFP is similarly fluorescent [Fig. 4(B), tube 7]. Collectively, these data show the nanobodies NB1 and pcNB1 are not appreciably fluorescent, and NB1 and pcNB1 are able to recover from thermal denaturation and bind GFP. Thus, polycationic resurfacing does not appreciably alter protein nanobody stability and robustness. Unsurprisingly, GFP lacking a His_6 tag does not have appreciable affinity for nickel-NTA [Fig. 4(B), tube 8].

Conclusions

In conclusion, the inability of most proteins to penetrate mammalian cells greatly limits the identification of new protein therapeutics that bind and modulate disease-relevant intracellular targets. Proteins with engineered solvent-exposed cationic features penetrate mammalian cells, but a lack in general guidelines for such extensive mutagenesis, and the inability to perform such extensive mutagenesis on a number of therapeutically-relevant proteins, limits the broader application of this approach. An alternative strategy is to identify a single protein scaffold that is amenable to polycationic resurfacing, is cell-penetrating, accesses the cytosol of mammalian cells, and can be evolved using *in vitro* or *in vivo* techniques to generate cell-penetrating proteins that bind and modulate

intracellular disease-relevant targets. Here, we show that three previously reported nanobodies can be resurfaced to display an extended polycationic feature on the framework region. This mutagenesis results in a new nanobody that is potently cell-penetrating, but structure, function, and stability/robustness is maintained. Based on these findings, we anticipate that polycationic resurfaced nanobodies might serve as a general scaffold for the discovery of protein basic research tools and therapeutic leads that target disease-relevant intracellular receptors. Efforts toward this goal are currently underway and will be reported in due course.

Methods

Cloning

All plasmids were constructed on a pETDuet-1 backbone. All proteins were assembled from a set of overlapping oligonucleotides. Proteins were amplified using vent and the constructs were ligated into *NdeI* and *NotI* restriction enzyme cleavage sites in the pETDuet-1 plasmid. Proteins containing GFP fusions were assembled from a set of overlapping oligonucleotides and ligated into *NdeI* and *KpnI* restriction enzyme cleavage sites in the pETDuet-1 plasmid.

Protein purification

Plasmids were transformed into BL21s (DE3). Cells were grown in either 2500 or 500 mL LB cultures containing carbenicillin at 37°C to $OD_{600} = \sim 0.6$ and induced with 1 m*M* IPTG at 25°C overnight. Cells were then collected by centrifugation and resuspended in either phosphate buffer with 150 m*M* NaCl for NBs (20 m*M* Sodium Phosphate, pH 7.4) or resuspended in phosphate buffer with 2*M* NaCl for pcNBs (20 m*M* Sodium Phosphate, pH 7.4) and stored at −20°C. Frozen pellets were thawed and incubated with complete ULTRA protease inhibitors tablets then sonicated for 2 min. The lysate was cleared by centrifugation (9000 rpm, 20 min) and the supernatant was mixed with 1 mL Ni-NTA agarose resin for 30 min. The resin was collected by centrifugation (4950 rpm, 10 min). The resin was washed with 50 mL buffer and 20 m*M* imidazole then 10 mL buffer and 50 m*M* imidazole. The protein was then eluted with 7 mL buffer containing 300 m*M* imidazole. The proteins were dialyzed against buffer and analyzed for purity by SDS-PAGE. Purified proteins were quantified using absorbance at 280 nm.

Circular dichroism

Proteins were purified as described above. Separately, each protein was diluted to 6–8 μM in Sodium Phosphate buffer (20 m*M* Sodium Phosphate, pH 7.4 and 150 m*M* NaCl). Wavelength data are the average of three scans from 250 to 200 nm in 1 nm steps at 25°C.

Mammalian cell culture

NIH/3T3 cells were cultured in Dulbecco's modified Eagle medium (DMEM) with 10% Fetal Bovine Serum (FBS). All cells were incubated at 37°C with 5% CO_2 environment.

Live cell fluorescence microscopy

Mammalian cells were grown to ~80% confluency in a six-well plate. Cells were then washed once with PBS and 2 mL of 250 nM protein fused with GFP was added. The cells were incubated with the protein solution for 3 h at 37°C, 5% CO_2 environment. After the incubation period, cells were washed once with PBS and three times with PBS-HS (heparin sulfate 20 U/mL) for 10 min at 37°C, 5% CO_2. The cells were then imaged on the EVOS FL fluorescence microscope.

Flow cytometry

Mammalian cells were grown to 80% confluency in a 6-well plate. Cells were then washed once with PBS and 2 mL of 10 nM, 250 nM, or 500 nM protein fused with GFP was added. The cells were incubated with the protein solution for 3 h at 37°C, 5% CO_2 environment. After the incubation period, cells were washed once with PBS and three times with PBS-HS (heparin sulfate 20 U/mL) for 10 min at 37°C, 5% CO_2. The cells were then removed from dish with 0.25% trypsin-EDTA and collected by centrifugation. The cells were then suspended in PBS and taken for flow cytometry analysis.

Cytosolic protein extraction and whole cell lysate preparation for Western blot

3T3 cells were plated in 6-well plate and grown to ~80% confluency. The cells were treated with 250 nM or 500 nM proteins (wtNB-GFP and pcNB-GFP or wtNB and pcNB, respectively) for 24 h at 37°C, 5% CO_2. After treatment, cells were washed once with PBS and once with PBS-HS (heparin sulfate 20 U/mL) for 10 min at 37°C, 5% CO_2 then lifted with 0.25% trypsin-EDTA and pelleted. For cytosolic protein extraction, cell pellets were resuspended in 100 μL of 50 μg mL^{-1} digitonin in 75 m*M* NaCl, 1 m*M* NaH_2PO_4, 8 m*M* Na_2HPO_4, 250 m*M* sucrose supplemented with Roche protease inhibitor cocktail for 10 min on ice. Cells were then centrifuged for 5 min at 13,000 rpm. Supernatant was then used as cytosolic protein extraction. Left over pellets were then re-suspended in 100 μL RIPA buffer supplemented with Roche protease inhibitor cocktail and incubated on ice for 5 min then further lysed through a 20 gauge needle. Supernatant was then used as whole cell lysate extraction. Both supernatants were collected and separated by

SDS-PAGE and transferred to a nitrocellulose membrane via an iBlot western blotting apparatus. The membrane was incubated in 1× TBS with 5% milk at 25°C for 1 h. The membrane was then washed three times with 1× TBS and 0.1% Tween-20. Primary antibodies for GFP, Erk1/2, and Rab5 were incubated with the membrane containing GFP fused nanobodies overnight in 10 mL of 1× TBS, 5% BSA, and 0.1% Tween-20 at 4°C. The western blot containing unfused nanobodies were incubated with primary antibodies for His_6, Erk1/2, and Rab5 overnight in same mixture. Both membranes were washed 3× with 1× TBS containing 0.1% Tween-20 and then incubated in Anti-Rabbit (Alexa Fluor 790) in 10 mL TBS, 5% milk and 0.1% Tween-20 for 1 h at 25°C. The membrane was washed 3× with 1× TBS containing 0.1% Tween-20 and imaged in 1× TBS using the Odyssey Classic Infrared Imager.

Ni-NTA pull-down assay

wtNB1 and pcNB1 (nanobodies for GFP) tagged with His_6 were cloned into MCS1 of pETDuet-1 using restriction enzymes *NcoI* and *NotI*. Untagged GFP was cloned into MCS2 of pETDuet-1 using restriction enzymes *NdeI* and *KpnI*. Completed constructs were transformed into BL21s (DE3). Cells containing the co-expressed pair were inoculated and induced as described previously. Cells were pelleted and purified as described previously. The pull-down was analyzed by SDS-PAGE.

Acknowledgment

The authors thank A. Chapman and S. Deporter (CSU) for the plasmid containing NB2 and Prof. S. Muyldermans (Vrije Universiteit Brussel) for generously providing a plasmid that encodes NB3.

References

1. Overington JP, Al-Lazikani B, Hopkins AL (2006) Opinion - how many drug targets are there? Nat Rev Drug Discov 5:993–996.
2. Smith GP, Petrenko VA (1997) Phage display. Chem Rev 97:391–410.
3. Esvelt KM, Carlson JC, Liu DR (2011) A system for the continuous directed evolution of biomolecules. Nature 472:499–U550.
4. Boder ET, Wittrup KD (2000) Yeast surface display for directed evolution of protein expression, affinity, and stability. Methods Enzymol 328:430–444.
5. DePorter SM, McNaughton BR (2014) Engineered M13 bacteriophage nanocarriers for intracellular delivery of exogenous proteins to human prostate cancer cells. Bioconjug Chem 25:1620–1625.
6. DePorter SM, Lui I, Bruce VJ, Gray MA, Lopez-Islas M, McNaughton BR (2014) Mutagenesis modulates the uptake efficiency, cell-selectivity, and functional enzyme delivery of a protein transduction domain. Mol Biosyst 10:18–23.
7. DePorter SM, Lui I, Mohan U, McNaughton BR (2013) A protein transduction domain with cell uptake and selectivity profiles that are controlled by multivalency effects. Chem Biol 20:434–444.
8. Torchilin V (2008) Intracellular delivery of protein and peptide therapeutics. Drug Discov Today Technol 5: e95–e103.
9. Fu A, Tang R, Hardie J, Farkas ME, Rotello VM (2014) Promises and pitfalls of intracellular delivery of proteins. Bioconjug Chem 25:1602–1608.
10. Stanzl EG, Trantow BM, Vargas JR, Wender PA (2013) Fifteen years of cell-penetrating guanidinium-rich molecular transporters: basic science, research tools, and clinical applications. Acc Chem Res 46:2944–2954.
11. Fuchs SM, Raines RT (2007) Arginine grafting to endow cell permeability. ACS Chem Biol 2:167–170.
12. Thompson DB, Cronican JJ, Liu DR (2012) Engineering and identifying supercharged proteins for macromolecule delivery into mammalian cells. Methods Enzymol 503:293–319.
13. Cronican JJ, Beier KT, Davis TN, Tseng JC, Li W, Thompson DB, Shih AF, May EM, Cepko CL, Kung AL, Zhou Q, Liu DR (2011) A class of human proteins that deliver functional proteins into mammalian cells in vitro and in vivo. Chem Biol 18:833–838.
14. Cronican JJ, Thompson DB, Beier KT, McNaughton BR, Cepko CL, Liu DR (2010) Potent delivery of functional proteins into Mammalian cells in vitro and in vivo using a supercharged protein. ACS Chem Biol 5: 747–752.
15. Muyldermans S (2013) Nanobodies: natural single-domain antibodies. Ann Rev Biochem 82:775–797.
16. Revets H, De Baetselier P, Muyldermans S (2005) Nanobodies as novel agents for cancer therapy. Expert Opin Biol Ther 5:111–124.
17. Kubala MH, Kovtun O, Alexandrov K, Collins BM (2010) Structural and thermodynamic analysis of the GFP:GFP-nanobody complex. Protein Sci 19:2389–2401.
18. Pardon E, Laeremans T, Triest S, Rasmussen SGF, Wohlkonig A, Ruf A, Muyldermans S, Hol WGJ, Kobilka BK, Steyaert J (2014) A general protocol for the generation of nanobodies for structural biology. Nat Protoc 9:674–693.
19. Abbady AQ, Al-Mariri A, Zarkawi M, Al-Assad A, Muyldermans S (2011) Evaluation of a nanobody phage display library constructed from a Brucella-immunised camel. Vet Immunol Immunopathol 142:49–56.
20. Sheikholeslami F, Rasaee MJ, Shokrgozar MA, Dizaji MM, Rahbarizadeh F, Ahmadvande D (2010) Isolation of a novel nanobody against HER-2/neu using phage displays technology. Labmedicine 41:69–76.
21. Saerens D, Pellis M, Loris R, Pardon E, Dumoulin M, Matagne A, Wyns L, Muyldermans S, Conrath K (2005) Identification of a universal VHH framework to graft non-canonical antigen-binding loops of camel single-domain antibodies. J Mol Biol 352:597–607.
22. Conrath KE, Lauwereys M, Galleni M, Matagne A, Frere JM, Kinne J, Wyns L, Muyldermans S (2001) Beta-lactamase inhibitors derived from single-domain antibody fragments elicited in the camelidae. Antimicrob Agents Chemother 45:2807–2812.
23. McNaughton BR, Cronican JJ, Thompson DB, Liu DR (2009) Mammalian cell penetration, siRNA transfection, and DNA transfection by supercharged proteins. Proc Natl Acad Sci USA 106:
24. Guilliams T, El-Turk F, Buell AK, O'Day EM, Aprile FA, Esbjorner EK, Vendruscolo M, Cremades N, Pardon E, Wyns L, Welland ME, Steyaert J, Christodoulou J, Dobson CM, De Genst E (2013) Nanobodies raised against monomeric alpha-synuclein

distinguish between fibrils at different maturation stages. J Mol Biol 425:2397–2411.
25. Appelbaum JS, LaRochelle JR, Smith BA, Balkin DM, Holub JM, Schepartz A (2012) Arginine topology controls escape of minimally cationic proteins from early endosomes to the cytoplasm. Chem Biol 19:819–830.
26. Rabideau AE, Liao XL, Pentelute BL (2015) Delivery of mirror image polypeptides into cells. Chem Sci 6:648–653.
27. Liao XL, Rabideau AE, Pentelute BL (2014) Delivery of antibody mimics into mammalian cells via anthrax toxin protective antigen. Chembiochem 15:2458–2466.